

# Calorimetric determination of the enthalpy change for the $\alpha$ -helix to coil transition of an alanine peptide in water

(L-alanine helix/peptide hydrogen bond/helix-coil enthalpy)

J. MARTIN SCHOLTZ\*, SUSAN MARQUEE\*†, ROBERT L. BALDWIN\*‡, EUNICE J. YORK§, JOHN M. STEWART§, MARCELO SANTORO¶, AND D. WAYNE BOLEN¶

\*Department of Biochemistry, Stanford University School of Medicine, Stanford, CA 94305; †Department of Biochemistry, University of Colorado Health Sciences Center, Denver, CO 80262; and ‡Department of Chemistry and Biochemistry, Southern Illinois University, Carbondale, IL 62901

Contributed by Robert L. Baldwin, December 7, 1990

**ABSTRACT** The enthalpy change ( $\Delta H$ ) accompanying the  $\alpha$ -helix to random coil transition in water has been determined calorimetrically for a 50-residue peptide of defined sequence that contains primarily alanine. The enthalpy of helix formation is one of the basic parameters needed to predict thermal unfolding curves for peptide helices and it provides a starting point for analysis of the peptide hydrogen bond. The experimental uncertainty in  $\Delta H$  reflects the fact that the transition curve is too broad to measure in its entirety, which precludes fitting the baselines directly. A lower limit for  $\Delta H$  of unfolding, 0.9 kcal/mol per residue, is given by assuming that the change in heat capacity ( $\Delta C_p$ ) is zero, and allowing the baseline to intersect the transition curve at the lowest measured  $C_p$  value. Use of the van't Hoff equation plus least-squares fitting to determine a more probable baseline gives  $\Delta H = 1.3$  kcal/mol per residue. Earlier studies of poly(L-lysine) and poly(L-glutamate) have given 1.1 kcal/mol per residue. Those investigations, along with our present result, suggest that the side chain has little effect on  $\Delta H$ . The possibility that the peptide hydrogen bond shows a correspondingly large  $\Delta H$ , and the implications for protein stability, are discussed.

Although it has the smallest side chain except for glycine, alanine has one of the highest helix propensities (1–4) of the amino acids in the genetic code: alanine-rich peptides as short as 16 residues form isolated  $\alpha$ -helices in water (1). This fact suggests that the  $\alpha$ -helix is an intrinsically stable structure in water and that larger side chains, as well as polar side chains, more often detract from helix stability than add to it. Studies with model compounds (5–8) have given differing estimates of the stability of the amide hydrogen bond in water but agree that competing hydrogen bonds to water drastically limit the stability of the amide hydrogen bond. Measurement of the enthalpy change ( $\Delta H$ ) and the heat capacity change ( $\Delta C_p$ ) for alanine helix formation should provide important information about the energetics of the peptide hydrogen bond, which is one of the fundamental constants of protein stability. We expect that the temperature-independent component of  $\Delta H$  should reflect the peptide hydrogen bond and van der Waals contacts, and the hydrophobic interactions will be reflected in  $\Delta C_p$ .

We report the calorimetric measurement of  $\Delta H$  for  $\alpha$ -helix formation by a 50-residue peptide, I, whose sequence is



The results give the enthalpy of formation of a monomeric helix of defined sequence and length. Short peptides give broad thermal unfolding transition curves and small heats of unfolding, whereas long polypeptides are difficult to synthesize and purify.

Compound I represents a compromise between these conflicting considerations. Synthesis of I began soon after the discovery that the sequence AEAAK, used as a repeating unit, forms stable helices when there are three repeats (9). The possible ion pairs formed by the  $\text{Glu}^-$ ,  $\text{Lys}^+$  residues with an  $i, i + 3$  spacing make only a minor contribution to helix stability; the major factor in helix formation is the high helix propensity of the alanine residues (1).

Calorimetric measurements of  $\Delta H$  have been reported for  $\alpha$ -helix formation by poly(L-glutamic acid) (10) and poly(L-lysine) (11), and noncalorimetric estimates of  $\Delta H$  have been reported for these and other polypeptides (ref. 12 and review in ref. 13). The theory of Zimm and Rice (14) has been used to take account of the ionization of poly(L-glutamic acid) and poly(L-lysine) (12, 13). These ionizable polypeptides form random coils when fully ionized and often aggregate when fully uncharged; thus, monomeric helix formation can be achieved only in conditions of partial ionization. A comparison of the value of  $\Delta H$  for alanine helix formation with those for lysine and glutamic acid, which have long ionizable side chains, should reveal whether the dominant contribution to  $\Delta H$  is made by the  $\alpha$ -helix backbone.

## MATERIALS AND METHODS

**Peptide Synthesis and Purification.** Peptide synthesis was performed on a Biosearch 9500 automatic synthesizer with stepwise solid-phase procedures (15) using a *tert*-butoxycarbonyl (Boc)/benzyl strategy and HF cleavage. *p*-Methylbenzhydramine (MBHA, polystyrene/1% divinylbenzene) resin was used to give the C-terminal amide. Double couplings and capping by acylation with acetylimidazole were employed routinely. A third coupling with a 1-hydroxybenzotriazole-benzotriazolylloxotris(dimethylamino)phosphonium hexafluorophosphate active ester (16) was used when monitoring by the qualitative Kaiser test showed the coupling to be incomplete. The synthesis was performed on a 0.4-mmol scale starting with Boc-Phe-MBHA resin. The crude peptide was purified first by gel filtration on Sephadex G-50 in 0.1 M acetic acid, then by reverse-phase HPLC on Vydac large-pore (300 Å)  $C_4$  resin with gradients of acetonitrile in 0.1% trifluoroacetic acid. Amino acid composition was determined with a Beckman 6300 amino acid analyzer after hydrolysis for 22 hr at 110°C in 6 M HCl.

**Circular Dichroism (CD) Measurements.** CD spectra were taken on an Aviv 60DS spectropolarimeter equipped with a Hewlett-Packard 89100A temperature control unit. Cuvettes with 10- or 1-mm pathlengths were employed. Ellipticity is

Abbreviations: DSC, differential scanning calorimetry;  $\Delta H_{\text{vH}}$ , van't Hoff enthalpy change;  $\Delta H_{\text{cal}}$ , calorimetric enthalpy change.

†Present address: Department of Biology, Massachusetts Institute of Technology, Cambridge, MA 02139.

‡To whom reprint requests should be addressed.

The publication costs of this article were defrayed in part by page charge payment. This article must therefore be hereby marked "advertisement" in accordance with 18 U.S.C. §1734 solely to indicate this fact.

reported as mean molar residue ellipticity,  $[\theta]$  ( $\text{deg}\cdot\text{cm}^2\cdot\text{dmol}^{-1}$ ), and was calibrated with (+)-10-camphorsulfonic acid (17). CD samples were prepared by diluting aqueous stock solutions of peptide either with 1 mM sodium citrate/1 mM sodium phosphate/1 mM sodium borate containing the indicated amount of NaCl or with 1 mM potassium phosphate containing KF. In either case the pH was adjusted with HCl and KOH or NaOH to pH 7.0 at room temperature. Stock peptide concentration was determined by measuring tyrosine absorbance in phosphate-buffered 6 M guanidine hydrochloride, pH 6.0, as described (1, 18).

**Differential Scanning Calorimetry (DSC).** Scanning calorimetry experiments were performed in degassed, pH 7.0, 1.0 mM phosphate buffer containing 0.1 M NaCl. The peptide concentration in the DSC cell was 1.72 mg/ml (0.366 mM) as determined by tyrosine absorbance (18). The experiments were performed with a MicroCal MC-2 differential scanning calorimeter (MicroCal, Northampton, MA) at a scanning rate of about  $1^\circ\text{C}/\text{min}$  under nitrogen pressure of 30 psi (206.7 kPa). Data analysis software was supplied by MicroCal and Ernesto Freire. For analysis, the raw data, in the form of heat flow ( $\text{mcal}\cdot\text{min}^{-1}$ ;  $1\text{ cal} = 4.184\text{ J}$ ) were converted to excess  $C_p$  ( $\text{kcal}\cdot\text{mol}^{-1}\cdot\text{K}^{-1}$ ) by dividing each data point of the thermal scan of peptide I by the scan rate ( $\text{K}\cdot\text{min}^{-1}$ ). The raw data from a thermal scan of buffer vs. buffer, also corrected for scan rate, were then subtracted. The resulting data were then divided by the number of moles of I contained in the sample cell to give the excess  $C_p$  scan for peptide I.

**DSC Data Analysis.** Because of the broad thermal transition of this peptide, it is not possible to determine the pre- and posttransition baselines necessary for a complete analysis of the calorimetric data. As a result, we are unable to determine  $\Delta C_p$  for the transition. To analyze the DSC data, we assumed  $\Delta C_p = 0$  and employed two strategies in handling the baseline problem.

The first strategy was to construct a baseline (or to "floor" the data) at the lowest excess  $C_p$  appearing in the scan and then fit the resulting set of data. This procedure provides an underestimate of the calorimetric enthalpy change ( $\Delta H_{\text{cal}}$ ), since the shape of the endotherm and the value of the van't Hoff enthalpy change ( $\Delta H_{\text{vH}}$ ) indicate that the endotherm is incomplete in the temperature range covered by the DSC data.

The second strategy involved an attempt to estimate the baseline  $C_p$  by means of a least-squares minimization procedure. Starting with the endotherm obtained by flooring the data to the lowest excess  $C_p$ , the baseline was systematically lowered by increments of  $50\text{ cal}\cdot\text{mol}^{-1}\cdot\text{K}^{-1}$ , and the data were fitted at each assumed baseline by setting  $\Delta C_p$  to zero while allowing  $\Delta H_{\text{cal}}$  and  $\Delta H_{\text{vH}}$  to float. The sum of the squares of the residuals (SSR) for each fit was recorded for each new baseline. The assumed  $C_p$  baseline resulting in the smallest SSR was taken as the best estimate of the baseline, and the corresponding values of  $\Delta H_{\text{vH}}$  and  $\Delta H_{\text{cal}}$  are reported as our best estimates of these thermodynamic parameters.

## RESULTS

**Peptide Design and Synthesis.** The sequence of the peptide used in these studies, I, is based upon one of the peptides first described by Marqusee and Baldwin (9). It is a longer version of their  $(i, i + 3)\text{E,K}$  peptide, which contains glutamic acid and lysine always separated by two alanine residues. There are eight blocks of the simple repeat AEAACA. The  $i, i + 3$  spacing of the glutamic and lysine residues was selected because side-chain interactions are minimal, when compared with the  $i, i + 4$  arrangement of the glutamic and lysine residues which stabilize the helix by forming intrahelical ion pairs. These stabilizing interactions have not been demonstrated with the  $(i, i + 3)\text{E,K}$  peptides. Since we wish to

investigate the thermodynamics of the helix-coil transition associated with the polypeptide backbone, we desire a peptide that contains minimal side-chain interactions. This peptide appears to be well suited for this purpose.

The peptide contains, in addition to the eight AEAACA repeats, blocked N- and C-terminal residues that eliminate the unfavorable interaction of the two charged termini with the helix macrodipole. The peptide also contains a single tyrosine residue, so that peptide concentration can be determined accurately by tyrosine absorbance (1, 18). Peptide purity was ascertained by reverse-phase HPLC on  $C_4$ ,  $C_{18}$ , and diphenyl resins to be  $>95\%$ , and amino acid analysis gave the expected composition. The molecular weight of the peptide was confirmed by fast atom bombardment mass spectrometry [calculated  $(M+H)^+$ , 4703.3; found, 4703.1  $\text{g}\cdot\text{mol}^{-1}$ ].

**CD Spectra.** The CD spectra of the peptide recorded at several different temperatures throughout the thermal transition between helix and coil are shown in Fig. 1. The low-temperature spectra are typical of those found for  $\alpha$ -helical peptides with minima at 222 and 208 nm and a maximum at 195 nm (19). The thermal transition shows an apparent isodichroic point at 202 nm, suggesting that all residues are either  $\alpha$ -helical or random-coil, with no alternative residue conformations.

**CD Thermal Unfolding Curves.** We measured the thermal unfolding curves of I by CD in order to determine the curve of percent helix versus temperature. This information provides a useful check on finding the correct baselines for the DSC experiments. The thermal unfolding curves of the peptide, measured by CD at 222 nm, are shown in Fig. 2 for several different peptide concentrations. The melting curves are superimposable, indicating that the peptide is monomolecular at these concentrations. Data obtained by heating and cooling experiments are identical, demonstrating the reversibility of the thermal transition from 0 to  $70^\circ\text{C}$ ; however, prolonged exposure of the peptide solution to temperatures  $>70^\circ\text{C}$  diminishes this reversibility. Both reversibility and monomolecularity are required for analysis of the thermodynamics of the helix-coil transition.

The difficulty of defining the CD baselines for the 100% helix and 100% coiled forms of the peptide limits our analysis of the transition. We investigated two different approaches to solving this problem. The first was to assume that the peptide is fully helical at  $0^\circ\text{C}$ , and to treat the helix-coil transition as a two-state reaction. The observed value for  $[\theta]_{222}$  at  $0^\circ\text{C}$  was then used together with a  $[\theta]_{222}$  value of 0 for the fully coiled form of the peptide to calculate the fraction helix at each temperature  $[f_H(T)]$  and  $\Delta H_{\text{vH}}$ . The second method used to

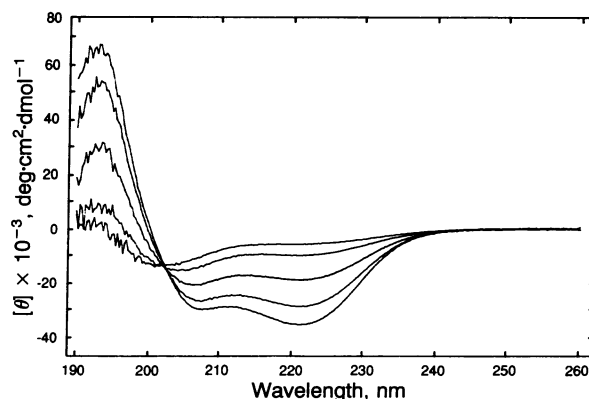


FIG. 1. CD spectra of peptide I recorded at temperatures in  $20^\circ\text{C}$  increments from  $0^\circ\text{C}$  (lowest curve at 222 nm) to  $80^\circ\text{C}$  (highest curve at 222 nm). The spectra were recorded at a peptide concentration of  $8.50\ \mu\text{M}$  in 1 mM potassium phosphate (pH 7.0) containing 0.1 M KF.

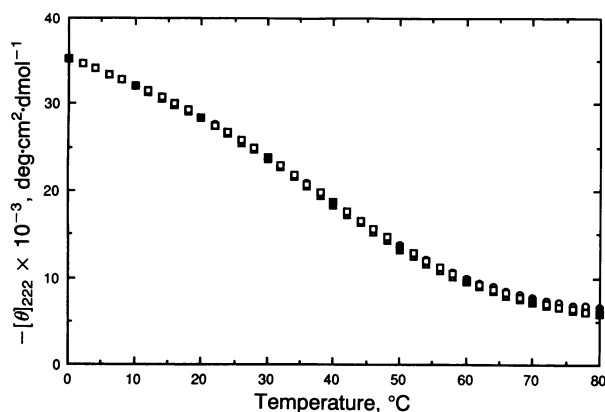


FIG. 2. Thermal unfolding curves for peptide I as monitored by CD. The concentrations of I for each experiment were 4.30  $\mu\text{M}$  ( $\Delta$ ), 8.60  $\mu\text{M}$  ( $\circ$ ), and 16.59  $\mu\text{M}$  ( $\square$ ). The solid points represent data obtained from cooling experiments on the same samples as indicated above.

derive  $\Delta H_{\text{vH}}$  from the CD thermal unfolding curves involved a least-squares fit of the observed  $[\theta]_{222}$  to the van't Hoff equation for a two-state process, allowing temperature-dependent CD baselines for both the fully helical  $\{[\theta]_{\text{H}}(T)\}$  and fully coiled  $\{[\theta]_{\text{C}}(T)\}$  forms of the peptide. The values calculated by the two methods are given in Table 1.

There are two primary reasons for calculating  $\Delta H_{\text{vH}}$ . The first is to find out whether a single value of  $\Delta H_{\text{vH}}$  is able to describe the observed thermal unfolding curve. If the fit is satisfactory, this  $\Delta H_{\text{vH}}$  value can be used to estimate, by extrapolation, the high-temperature and low-temperature regions of the curve, which cannot be measured directly. The second is to compare the  $\Delta H_{\text{vH}}$  values calculated from CD and DSC; if the two values are the same, it implies that each technique is monitoring the same temperature-dependent process, regardless of the validity of the two-state assumption.

**DSC.** The broad DSC endotherm observed for peptide I creates a number of technical difficulties in evaluation of  $\Delta H_{\text{vH}}$  and  $\Delta H_{\text{cal}}$  associated with the thermal transition. Analysis of the thermal transition curves, therefore, requires knowledge of the initial and final portions of the transition, in addition to information about the thermal baseline within the transition zone.

We used two approaches to estimate the baseline in the DSC scans. The first method, in which a flat baseline was constructed by requiring the baseline to intersect the endotherm at the lowest  $C_p$ , does a poor job of fitting the data at high temperatures, suggesting the endotherm is incomplete in this temperature range (data not shown). This procedure truncates the data, and consequently this approach underestimates  $\Delta H_{\text{cal}}$ ; values of  $\Delta H_{\text{cal}}$  and  $\Delta H_{\text{vH}}$  obtained in this way are given in Table 2.

One interpretation of the poor fit at high temperatures is that effects of irreversibility begin above 70°C and might be responsible for the aberrant fit. Accordingly, we truncated the data at 75°C and considered another approach to defining

Table 1.  $\Delta H_{\text{vH}}$  determined from CD data

Method	$[\theta]_{\text{H}}(T)^*$	$[\theta]_{\text{C}}(T)^*$	$\Delta H_{\text{vH}}$ , kcal·mol <sup>-1</sup>	
			Per peptide	Per residue
1	-35,200	0	11.4	0.23
2	103T - 40,000	-46T + 640	11.0	0.22

\*Values for the fully helical form,  $[\theta]_{\text{H}}(T)$ , and fully coiled form,  $[\theta]_{\text{C}}(T)$ , of the peptide are expressed in deg·cm<sup>2</sup>·dmol<sup>-1</sup> with T in °C. The two methods used to calculate  $\Delta H_{\text{vH}}$  are described in *Materials and Methods*.

Table 2. Helix-coil  $\Delta H$  values determined from DSC data

Sample	$\Delta H_{\text{cal}}$ , kcal·mol <sup>-1</sup>		$\Delta H_{\text{vH}}$ , kcal·mol <sup>-1</sup>	
	Per peptide	Per residue	Per peptide	Per residue
1*	45.8	0.92	13.8	0.28
2*	40.5	0.81	14.0	0.28
1†	67.6	1.35	11.0	0.22
2†	60.0	1.20	11.3	0.23

Values were obtained by fitting DSC scans to the 50-mer, assuming  $\Delta C_p = 0$  while allowing  $\Delta H_{\text{cal}}$  and  $\Delta H_{\text{vH}}$  to float.

\*The baseline was imposed by "flooring" the DSC data such that the baseline intersects the DSC data at the point of lowest excess  $\Delta C_p$  (viz., at 90°C).

†The baseline for this fitting was arrived at by truncating the data at 75°C and successively lowering the "floored" baseline to obtain the baseline giving a minimum in the sum of squares of residuals for fitting (see *Materials and Methods*). An example of the fitted data is given as a solid line in Fig. 3.

the most probable baseline. The baseline was successively lowered in  $C_p$  increments of 50 cal·mol<sup>-1</sup>·K<sup>-1</sup> and a fitting was performed for each new baseline, assuming  $\Delta C_p = 0$  and allowing  $\Delta H_{\text{cal}}$  and  $\Delta H_{\text{vH}}$  to float. When the sum of squares of the residuals for each fitting reached a minimum, the baseline  $C_p$  at that minimum was taken as the most probable baseline. Fig. 3 presents the best fit of the data, using this as the most probable baseline. Table 2 provides the best-fit values for  $\Delta H_{\text{cal}}$  and  $\Delta H_{\text{vH}}$  using this baseline. The  $\Delta H_{\text{vH}}$  values determined by CD (Table 1) and by DSC (Table 2) agree satisfactorily, indicating that the spectroscopic and calorimetric probes are monitoring the same temperature-dependent process.

## DISCUSSION

**Enthalpy of  $\alpha$ -Helix Formation in Water.** The alanine-based  $\alpha$ -helix forms a stable structure in water because of the favorable enthalpy of helix formation. The present study places  $\Delta H_{\text{cal}}$  of  $\alpha$ -helix formation in the neighborhood of -1 kcal per mol per residue (Table 2). This result supports the explanation for the high helix-forming propensity of alanine (2) in which the  $\alpha$ -helix backbone is stable in water.

The broad thermal unfolding transition, observed by both CD and DSC measurements, is typical for small helical peptides. The broadness of the transition precludes any analysis of the  $\Delta C_p$  for helix formation and forces us to evaluate  $\Delta H$  without the benefit of well-defined baselines. The two methods of applying baselines to the DSC scans provide practical ranges for  $\Delta H_{\text{cal}}$  accompanying the helix-coil transition. Simply flooring the DSC data to the smallest  $C_p$  of the scan and integrating the area under the curve gives a lower limit for  $\Delta H_{\text{cal}}$  of 43 kcal per mol of peptide. Use of a systematic least-squares procedure for determining the baseline of the DSC scans gives an estimate for  $\Delta H_{\text{cal}}$  of 64 kcal per mol of peptide. Thus, the helix-coil  $\Delta H$  per residue is a minimum of 0.86 kcal per mol, with the best estimate of  $\Delta H_{\text{cal}}$  being around 1.3 kcal per mol per residue.

Calorimetric measurements of  $\Delta H$  for the helix-coil transition in water have been reported for two ionizable polypeptides: poly(L-glutamic acid) (10) and poly(L-lysine) (11). Both studies place  $\Delta H$  for helix formation in the neighborhood of -1.1 kcal per mol per residue, after correction for the heat of ionization of the side chains. The polypeptides containing either L-glutamate or L-lysine form  $\alpha$ -helices only under conditions of partial ionization; the fully charged forms are not helical, whereas the uncharged forms aggregate. It is only under conditions of partial ionization that either of these polypeptides adopts a helical structure. This places restrictions on the experimental conditions available and necessitates correcting the observed  $\Delta H$  for the ionization of the side

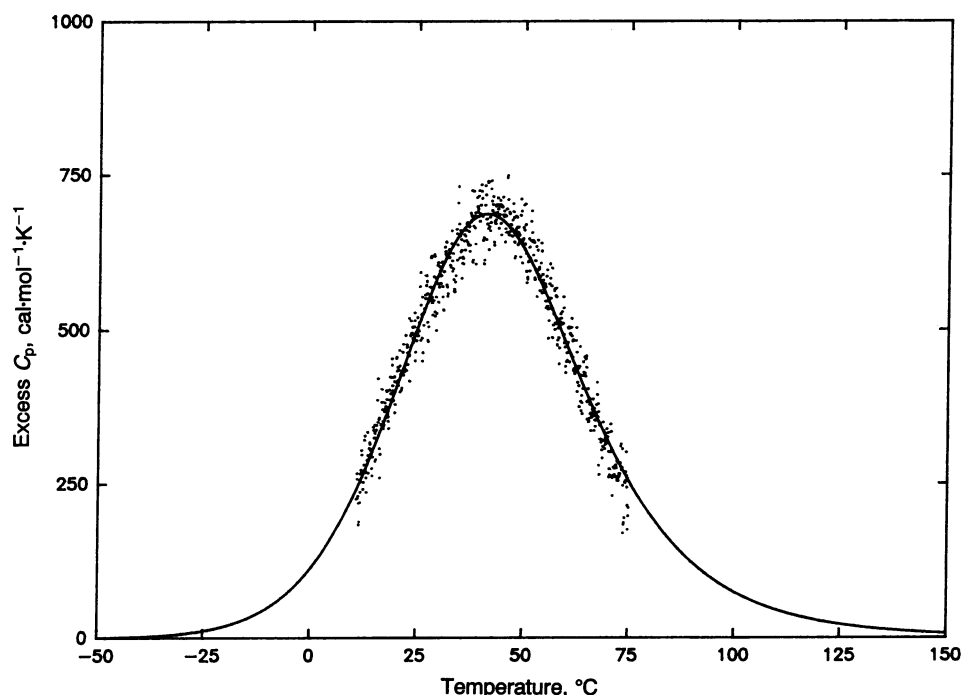


FIG. 3. DSC scan for peptide I, truncated at 75°C to avoid complications from irreversibility. The peptide concentration was 1.72 mg/ml in 1 mM potassium phosphate (pH 7.00) containing 0.1 M NaCl. The baseline used was determined using the second procedure described in *Materials and Methods*. The solid curve was generated using parameters from Table 3;  $\Delta H_{vH} = 11.3$  kcal per mol of peptide,  $\Delta H_{cal} = 60.0$  kcal per mol of peptide.

chains. In spite of the differences between poly(L-glutamate), poly(L-lysine), and the L-alanine-based peptide, each calorimetric study gives essentially the same value for the enthalpy of helix formation in water, indicating that  $\Delta H$  is determined chiefly by main-chain interactions.

The theory of the  $\alpha$ -helix-random coil transition, which is based on a statistical mechanical model for helix formation, shows that the helix-coil transition is not a two-state reaction, even for short peptides. For  $\alpha$ -helix formation by an infinite-chain polypeptide, the  $\Delta H_{cal}/\Delta H_{vH}$  ratio is found to be  $\sigma^{-1/2}$  (20), where  $\sigma$  is the nucleation constant (in the range of  $10^{-3}$  to  $10^{-4}$ ; see refs. 13 and 14) and  $\sigma^{-1/2}$  can be thought of as the length of the cooperative unit. For shorter peptides,  $\Delta H_{cal}/\Delta H_{vH}$  is a function of chain length, and values of  $\Delta H_{vH}$  that are smaller than  $\Delta H_{cal}$  are expected for all chain lengths. We have confirmed this basic prediction of helix-coil transition theory, that  $\Delta H_{cal} \gg \Delta H_{vH}$  (and therefore that  $\alpha$ -helix formation is far from being a two-state reaction), by our measurements of  $\Delta H_{cal}$  and  $\Delta H_{vH}$  (Table 2).

**Comparison of the  $\Delta H$  of Helix Formation with Model Compound Studies.** There have been several studies of the formation in water of dimers, and possibly also higher oligomers, of compounds such as urea (5), *N*-methylacetamide (6), and  $\delta$ -valerolactam (7) that might be held together by amide hydrogen bonds. There is general agreement that the dimers formed are weak and that the net strength of the amide hydrogen bond in water must be quite weak. There is disagreement, however, about whether specific dimer formation is observed at all and whether amide hydrogen bonds are responsible for dimer formation. Moreover, the model compound studies give differing estimates of  $\Delta H$  of the amide hydrogen bond in water.

Schellman (5) used accurate literature data for the heat of dilution of urea solutions to show that urea dimer formation is likely and that  $\Delta H$  of dimer formation corresponds to  $-1.5$  kcal per mol per putative amide hydrogen bond. Schönert and Stroth (21) found that binding of urea to simple peptides has similar thermodynamic properties to the urea dimer studied by Schellman; they pointed out, however, that uncertainty in estimating small dimerization constants has a large effect on the estimated  $\Delta H$ . Further studies of the urea dimer system by Barone *et al.* (22) gave results consistent with Schellman's original estimate. Dimeric lactams, which

show stronger association and might be held together by two amide hydrogen bonds, have been studied by Susi *et al.* (7, 23). A complicating feature of the results for lactam dimers, as noted by Susi and Ard (23), is that "dimerization" of  $\epsilon$ -caprolactam is not a two-state reaction, and they suggested that hydrophobic interactions might be involved in driving its association.

Another model compound study, which may be more applicable to strictly aqueous solution, comes from Suri *et al.* (8). By measuring the second virial coefficients for interaction between several pairs of solutes in water, and by interpreting the results with a group additivity principle, they found a significant attractive interaction between NH and CO groups in water; they limited their studies to moderately dilute solutions ( $\leq 1$  M) in order to obtain results characteristic of aqueous solution. This precaution is not feasible in the other model compound studies cited above.

In addition to the model compound studies designed to estimate the strength of the amide hydrogen bond in water, there have also been theoretical treatments of the problem (24, 25). In a molecular dynamics simulation of the association of *N*-methylacetamide in water, Jorgensen (24) found that association is driven by a dipolar interaction, not by formation of amide hydrogen bonds. Sneddon *et al.* (25) used a similar simulation method to study the interaction between two formamide molecules in water and in an apolar solvent. They found that the hydrogen-bonded dimer is more stable in water than in an apolar solvent, but the Gibbs energy of amide hydrogen bond formation in water is roughly zero. These results illustrate the problems of using model compounds and studies of dimer formation to investigate the properties of the amide hydrogen bond in water. In contrast, peptide  $\alpha$ -helix formation is a monomolecular reaction that can be studied in dilute solution and yields several peptide hydrogen bonds formed for each helical molecule.

One particularly germane theoretical treatment of the stability of the  $\alpha$ -helix in water comes from Ooi and Oobatake (26). Using parameters derived from the thermodynamics of protein unfolding and from model compound studies of the effects of water on the unfolded and folded forms of a protein, they are able to predict  $\Delta H$  and its temperature dependence for an isolated alanine  $\alpha$ -helix in water. Their results suggest that helix formation is enthalpy-driven, and the predicted  $\Delta H$

for unfolding of a 40-residue alanine helix (0.86 kcal per mol per residue) is close to the  $\Delta H_{\text{cal}}$  we observe for our peptide. They are also able to estimate the temperature dependence of  $\Delta H$  (that is,  $\Delta C_p$ ). They predict that  $\Delta C_p$  is small (2.0 cal per mol of residue per K), and that the major contribution to the large  $\Delta H$  for helix formation is temperature-independent. Their work suggests that hydrogen bond formation and van der Waals contacts should be the dominant factors stabilizing the  $\alpha$ -helix. Further work is needed to test this prediction.

**Implications for Protein Folding and Structure.** One of the fundamental constants of protein stability is the strength of the peptide hydrogen bond in water. For a typical globular protein, the majority of the backbone amides are involved in hydrogen-bonding interactions in the folded protein, and most of these amides are fully solvated in the unfolded protein. Our results place  $\Delta H$  for helix formation in the neighborhood of  $-1$  kcal per mol per residue. It appears that the major contribution to this  $\Delta H$  comes from the peptide backbone itself, which suggests the enthalpy of the peptide hydrogen bond is substantial. Even if this enthalpic contribution to the stability of the folded protein is unique to the  $\alpha$ -helix,  $-1$  kcal per mol per residue would still represent a major factor in the stability of protein structure. Further work is required to analyze the factors contributing to  $\Delta H$  for  $\alpha$ -helix formation and to determine whether the peptide hydrogen bonds found in  $\beta$ -sheets and  $\beta$ -turns also show large values of  $\Delta H$ .

We thank the National Institutes of Health Clinical Mass Spectrometry Resource, University of Colorado, supported by Grant RR01152, and the Massachusetts Institute of Technology Mass Spectrometry Facility, supported by National Institutes of Health Center for Research Resources Grant RR00316, for the fast atom bombardment mass spectra. We thank Robert J. Binard for amino acid analysis and Doug Barrick, Hong Qian, and John Schellman for critical review of the manuscript. J. M. Scholtz is a Public Health Service Postdoctoral Fellow (GM13451). S.M. acknowledges support from the National Institutes of Health Medical Scientist Training Program (GM7365). This work was supported by grants from the National Institutes of Health (GM31475) and National Science Foundation (DMB 8904394) to M.S. and D.W.B.

1. Marqusee, S., Robbins, V. H. & Baldwin, R. L. (1989) *Proc. Natl. Acad. Sci. USA* **86**, 5286–5290.
2. Padmanabhan, S., Marqusee, S., Ridgeway, T., Laue, T. M. & Baldwin, R. L. (1990) *Nature (London)* **344**, 268–270.
3. Ihara, S., Ooi, T. & Takahashi, S. (1982) *Biopolymers* **21**, 131–145.
4. Takahashi, S., Kim, E.-H., Hibino, T. & Ooi, T. (1989) *Biopolymers* **28**, 995–1009.
5. Schellman, J. A. (1955) *C. R. Trav. Lab. Carlsberg* **29**, 223–229.
6. Klotz, I. M. & Franzen, J. S. (1962) *J. Am. Chem. Soc.* **84**, 3461–3466.
7. Susi, H., Timasheff, S. N. & Ard, J. S. (1964) *J. Biol. Chem.* **239**, 3051–3054.
8. Suri, S. K., Spitzer, J. J., Wood, R. H., Abel, E. G. & Thompson, P. T. (1985) *J. Solution Chem.* **14**, 781–794.
9. Marqusee, S. & Baldwin, R. L. (1987) *Proc. Natl. Acad. Sci. USA* **84**, 8898–8902.
10. Rialdi, G. & Hermans, J. (1966) *J. Am. Chem. Soc.* **88**, 5719–5720.
11. Chou, P. Y. & Scheraga, H. A. (1971) *Biopolymers* **10**, 657–680.
12. Hermans, J. (1966) *J. Phys. Chem.* **70**, 510–515.
13. Ptitsyn, O. B. (1972) *Pure Appl. Chem.* **31**, 227–244.
14. Zimm, B. H. & Rice, S. A. (1960) *Mol. Phys.* **3**, 391–407.
15. Stewart, J. M. & Young, J. D. (1984) *Solid Phase Peptide Synthesis* (Pierce, Rockford, IL).
16. Hudson, D. (1988) *J. Org. Chem.* **53**, 617–624.
17. Chen, G. C. & Yang, J. T. (1977) *Anal. Lett.* **10**, 1195–1207.
18. Brandts, J. F. & Kaplan, L. J. (1973) *Biochemistry* **12**, 2011–2024.
19. Woody, R. W. (1985) in *The Peptides*, eds. Udenfriend, S., Meienhofer, J. & Hruby, J. R. (Academic, New York), Vol. 7, pp. 15–114.
20. Applequist, J. (1963) *J. Chem. Phys.* **38**, 934–941.
21. Schönert, H. & Stroth, L. (1981) *Biopolymers* **20**, 817–831.
22. Barone, G., Castronuovo, G., Del Vecchio, P. & Giancola, C. (1989) *J. Chem. Soc. Faraday Trans. 1* **85**, 2087–2097.
23. Susi, H. & Ard, J. S. (1969) *J. Phys. Chem.* **73**, 2240–2241.
24. Jorgensen, W. L. (1989) *J. Am. Chem. Soc.* **111**, 3370–3371.
25. Sneddon, S. F., Tobias, D. J. & Brooks, C. L. (1989) *J. Mol. Biol.* **209**, 817–820.
26. Ooi, T. & Oobatake, M. (1991) *Proc. Natl. Acad. Sci. USA* **88**, 2859–2863.